24th INTERNATIONAL CONGRESS ON SOUND AND VIBRATION
23–27 July 2017, London

ICSV24
23-27JULY 2017
LONDON CALLING

NUMERICAL SIMULATION AND EXPERIMENTAL VALIDATION OF NORMAL STRAIN DISTRIBUTION AND PITTING PHENOMENON IN INDUSTRIAL GEARS

Matteo Strozzi

University of Ferrara, Department of Engineering, Ferrara, Italy
email: strmtt@unife.it

Marco Barbieri, Antonio Zippo, Francesco Pellicano

University of Modena and Reggio Emilia, Department of Engineering "Enzo Ferrari", Modena, Italy

In this paper, the normal strain distribution and pitting phenomenon on gears are investigated by means of numerical finite element analyses and experimental activities. In the first part of the paper, results of experimental tests for the investigation of the pitting phenomenon on gears are reported. These durability tests are made at a specific nominal load and far from the resonance. The experimental data are collected periodically from two tri-axial accelerometers placed on the gear shafts. After a short time, a visible pitting phenomenon arises on the gear teeth, where the contact pattern is perfectly centered (due to the high lead crown imposed on the teeth) and the wear pattern is consistent with FE simulations. In the second part of the paper, numerical finite element studies on the normal strain distribution at the base of the gear teeth during the contact are reported. These analyses are made at the same nominal load of the previous pitting analyses and at very low rotational speed (static analyses). A peak of normal strain at the base of the contact tooth is found around the contact time, preceded and followed by a low constant value of normal strain. The numerical results are validated by comparisons with experimental tests carried out in the same operating conditions and placing strain gauges at the tooth base of the gears.
Keywords: normal strain, pitting, gears

1. Introduction

Gear teeth are subjected to high contact pressures and fatigue loads in operating conditions [1-2].

Therefore, the analysis of the effect of the surface pitting and wear on the vibration of a gear transmission system, together with the investigation of the pressure and normal strain distributions, can be applied to deeply improve the mechanical properties of the gearbox [3-5]. Other relevant studies on the nonlinear dynamics effects of mechanical systems can be found in Refs. [6-10].

In the present paper, experimental tests and FEM analyses of pitting and normal strain distribution in industrial gears are performed.

In the experimental measurements, an overload in terms of applied torque is used to exert excessive stresses on the gear teeth and produce pitting in undamaged gears under non-stationary conditions within a short time. The experimental data are collected periodically from tri-axial accelerometers placed on the gear shafts. FE simulations are performed to verify contact and wear patterns.

The normal strain distribution at the base of the gear teeth during the contact is studied by means of FE analyses. A peak of normal strain at the base of the contact tooth is found around the contact time, preceded and followed by low constant value of normal strain. The numerical results are validated by means of comparisons with experimental tests carried out by placing strain gauges at the root fillet of six consecutive teeth of each gear.

2. Pitting phenomenon

In this section, the experimental activities performed by means of accelerated endurance tests in order to investigate the pitting phenomenon on gears are reported. The test rig used in the experimental activities is an open-loop configuration experiment designed for testing single gear pairs, with maximum torque of 200Nm and maximum rotational speed of 3000RPM. Two DC motors are present, one of them acts as a motor and the second has the role of electric brake (generator); the controller allows an internal electric energy recirculation. The test rig allows to test single spur gear pairs with arbitrary centre distance and the possibility of two angular misalignments. Two torque-meters measure the applied input and output torque, while four tangential rotating accelerometers measure the rotational vibration of the wheels and consequently the dynamic transmission error.

2.1 Experimental setup

The test bench is represented in Figure 1, two gears are mounted on shafts connected to two DC motors (engine + brake), these are highly balanced motors characterized by very low torque ripple.

Starting from the motor on the left of Figure 1, and moving to the right, one finds: i) a flywheel; ii) an elastic joint (Falk Steelflex T10" model 1050T); iii) a torque-meter; iv) an hollow super-stiff shaft mounted on two roller bearings, where the bearings are connected on a very stiff foundation.

The test bench can simulate and monitor the dynamic behaviour of a gear pair. The structure is constituted by two hollow shafts supported by two casings on which flanges are connected through screws. The possibility to mount the wheels on the shafts individually simulating the operation of a reduction gear represents a great advantage compared to the case in which it has to handle gearbox. In this way, it can be continuously monitored by the use of mounted accelerometers.

A specific activity was carried out in order to design a special gear pair undergoing to a fast pitting phenomena with maximum available torque (DC engines) of 200Nm, where at the same time the bending failures must be avoided. This was reached by introducing a large amount of crowning along the face width. The goal was to obtain a gear pair so that the pitting can be found within 60 hours. Precise data on the steel and surface finishing are needed for a proper estimate of pitting.

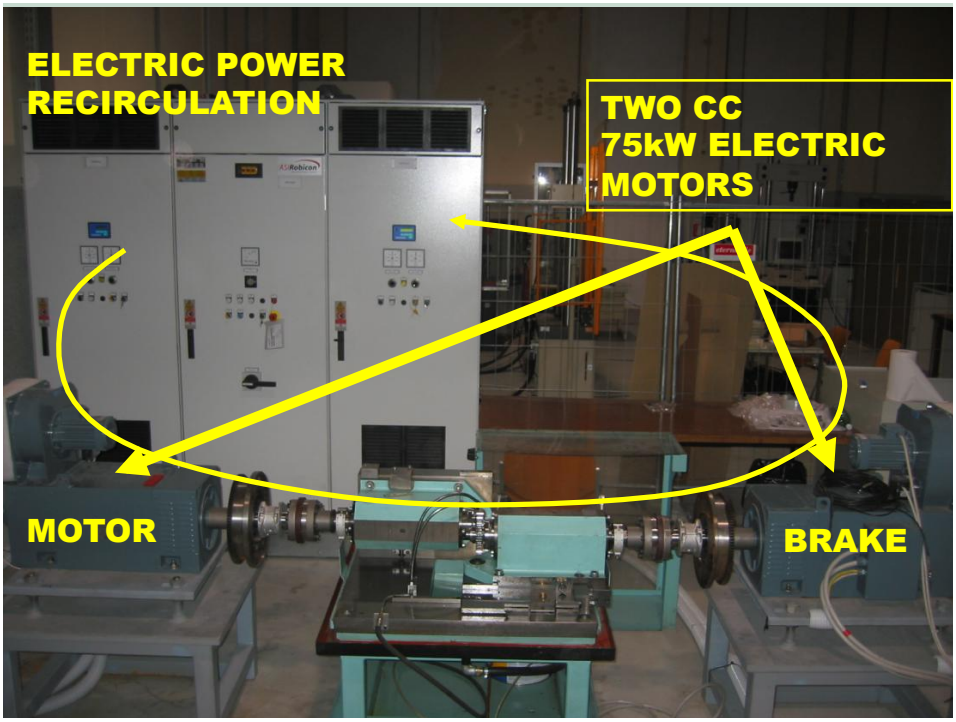

Figure 1: Test rig for the laboratory experiments.

2.2 Pitting tests

The pitting tests were made at nominal load of 130Nm, which was found to be far from the resonance, and the chosen rotational frequency was 840RPM.

The signals were collected by two tri-axial accelerometers on pinion and gear shaft supports respectively and by two uni-axial accelerometers on motor side and on brake side.

In Figure 2, a picture of the pinion with the teeth numbering is reported.

After a 4 hours test at external torque 130Nm, speed 840RPM and external temperature 20°C, a visible pitting phenomenon was given, with the presence of two craters on the side of two adjacent teeth of the pinion, together with several smaller pits.

The pitting phenomenon was present in four teeth (4,8,9,12), where for each pitted tooth the pitting size was estimated as a percentage of the total flank area 1.42cm^2 (the pitting sizes are 3.3%, 4.4%, 2%, 1.1%, respectively), see Figures 3-6.

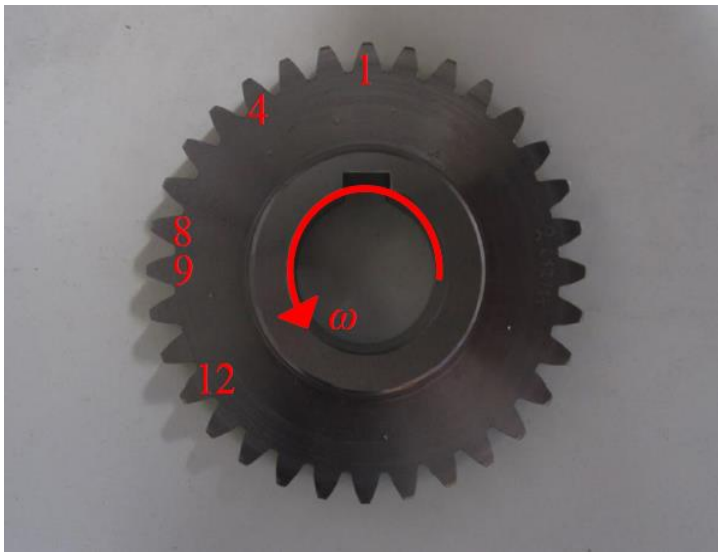

Figure 2: Teeth numbering of the pinion.

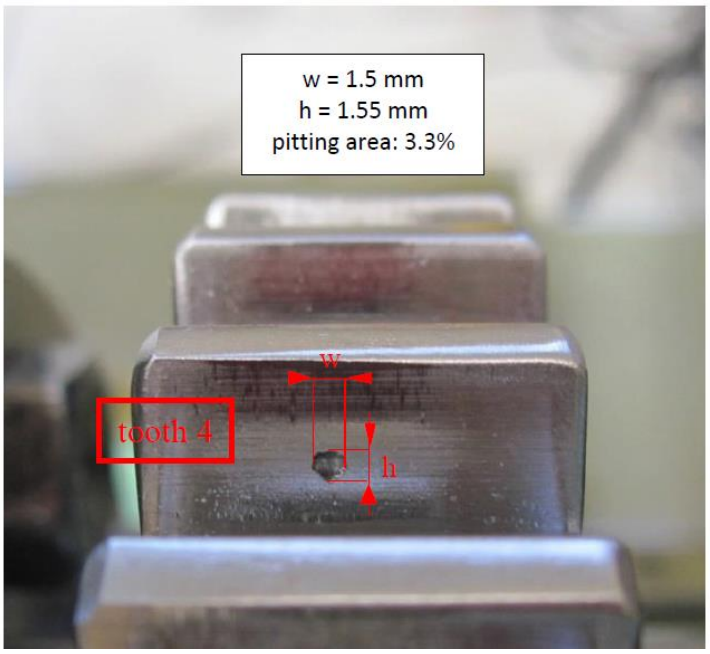

Figure 3: Pitting on tooth 4 of the pinion.

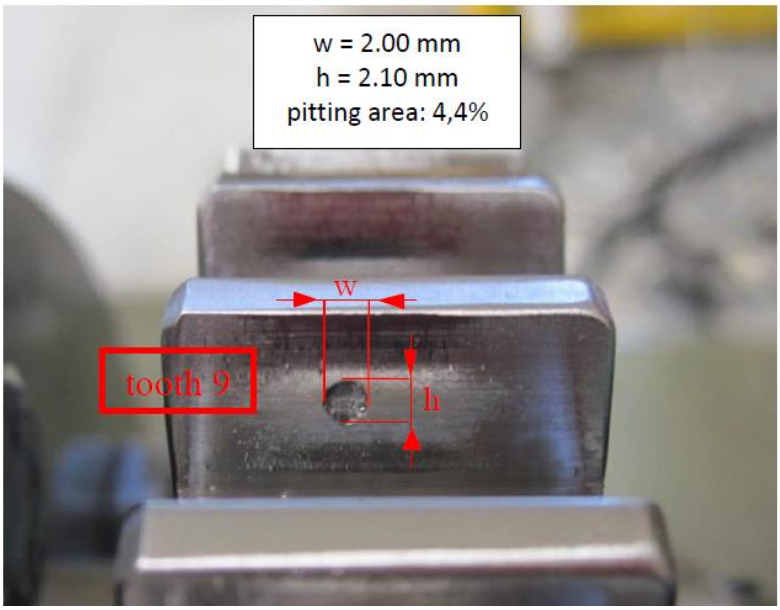

Figure 4: Pitting on tooth 9 of the pinion.

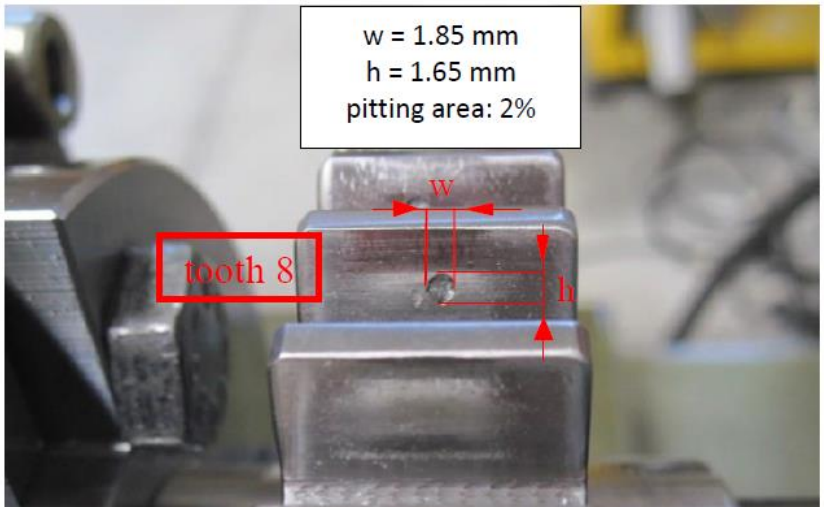

Figure 5: Pitting on tooth 8 of the pinion.

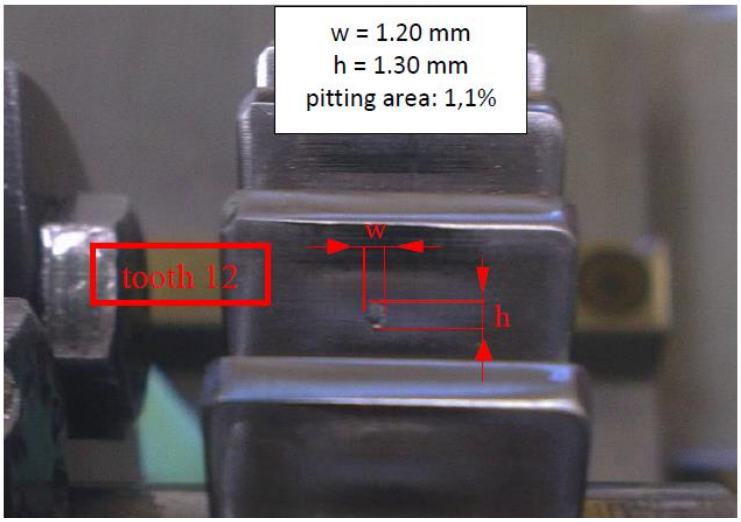

Figure 6: Pitting on tooth 12 of the pinion.

3. Normal strain distribution

In this section, the numerical studies performed by means of finite element analyses to investigate the normal strain distribution on the gear teeth are reported. The numerical results are validated by means of comparisons with experimental tests carried out applying strain gauges at the root fillet of six consecutive teeth of each gear.

3.1 Numerical simulations

The FEM modelling of the test rig was carried out using the numerical software Calyx® (Transmission3D), which allows to build up the multi-body finite element model and investigate stresses and strains of the different elements of the mechanical system.

The FEM modelling of the overall mechanical system (pinion, gear, shafts, bearings) is shown in Figure 7; the mechanical system is given by pinion rotor (sun: 32 teeth, shaft: 15 segments, bearing inner race: 6 sectors), gear rotor (sun: 39 teeth, shaft: 15 segments, bearing inner race: 6 sectors), ground (bearing outer race: 12 sectors) and bearings (pinion: 2 sectors × 15 rollers + 4 sectors × 17 rollers, gear: 4 sectors × 17 rollers + 2 sectors × 15 rollers).

In the present dynamic analyses, the external torque is applied to the pinion (right hand), while the rotational frequency is applied to the gear (left hand); the displacement constrains (u,v,w) = 0 are imposed to the pinion, while the displacement constrains (u,v,w) = 0 and rotational constraints ($\theta x,\theta y,\theta z$) = 0 are imposed to the gear.

The numerical FE studies on the normal strain distribution at the base of the gear teeth during the contact are reported in Figure 8. These analyses were made at the same nominal load of the previous pitting analyses (130Nm) and at very low rotational speed (10RPM). From this Figure, it can be seen that a peak of normal strain at the base of the contact tooth is found around the contact time (from -1.5 to 0.0), preceded and followed by a low constant value of normal strain. The normalized time is given along the x-axis (from -3 to +3), where the micro-strains με are given along the y-axis. The minimum peak is equal to -240με, the maximum peak is equal to +220με.

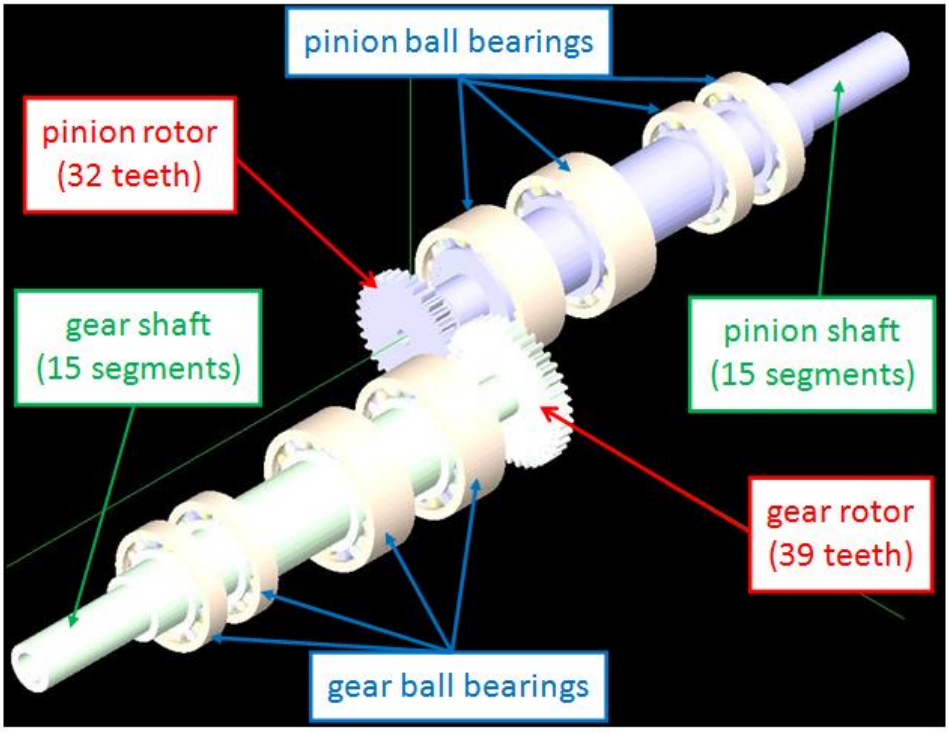

Figure 7: FEM modelling of the mechanical system (pinion, gear, shafts, bearings).

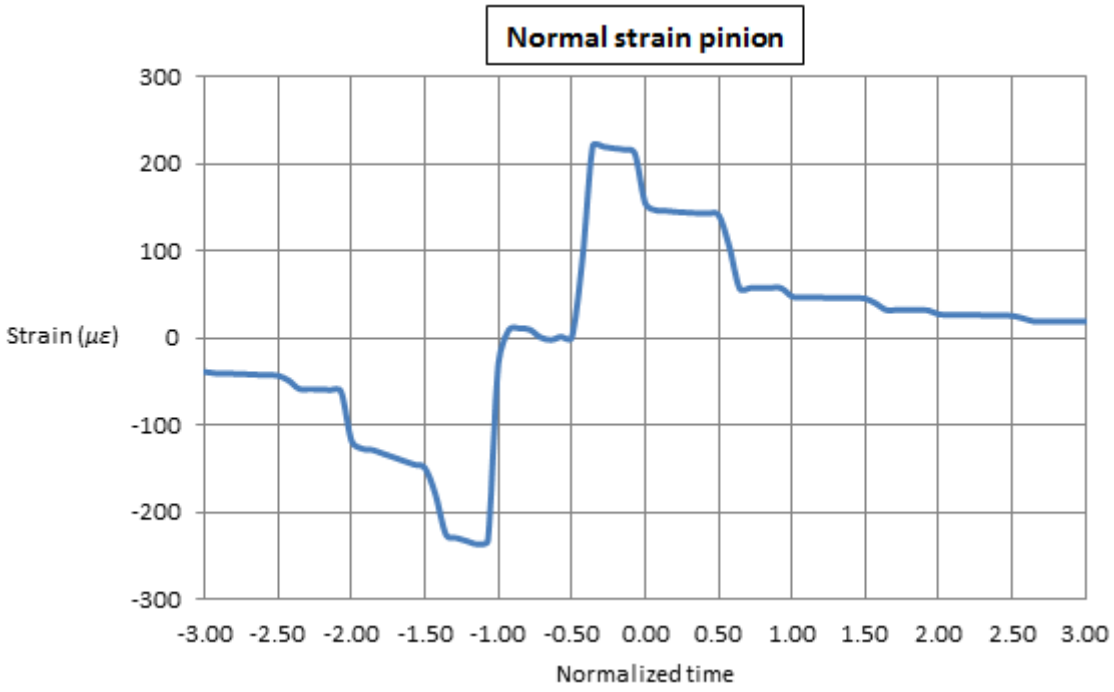

Figure 8: FEM normal strain vs. normalized time at the base of tooth 25 of the pinion rotor.

3.2 Experimental validation

In order to validate the previous FE analyses on the normal strain distribution at the tooth base, a comparison with experimental results is presented. The experimental test was performed at the same operating conditions of the FE analyses (130Nm nominal load, 10RPM rotational speed); six strain gauges were applied at the root fillet of six consecutive teeth of each gear, see Figure 9.

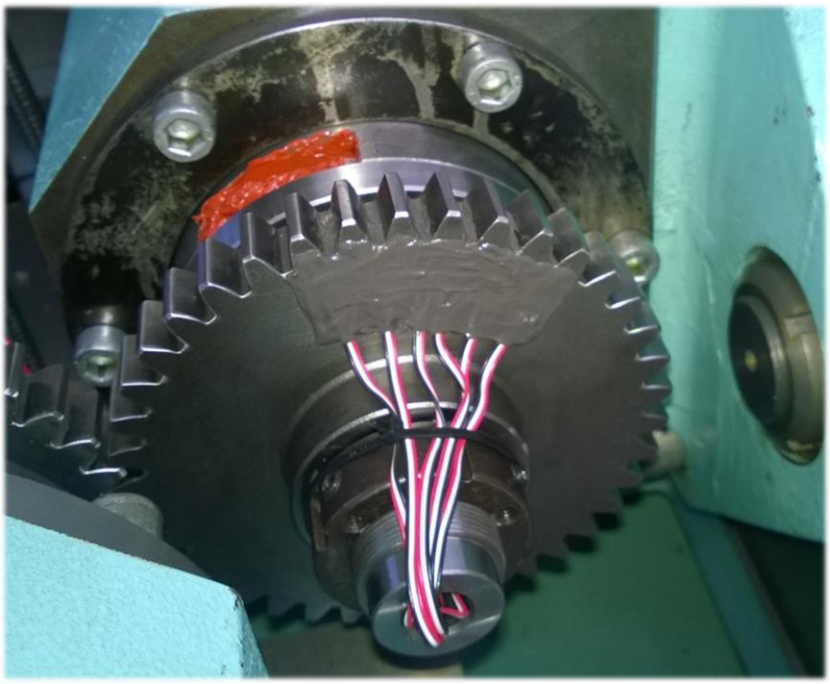

Figure 9: Strain gauge details of gears connections.

The acquisition data system was connected with the strain gauges on the two gears to continually monitor the normal strains; a silicon layer covers the sensors to protect them from the lubricant oil.

The strain gauges Vishay 06-015EH-EA-120 have been used, presenting the following features: resistance 120ohms ± 0.3%, length 0.38mm, width 0.48mm, maximum operating temperature 150-200°C; the strain gauges were mounted rotated by 90°, looking at the wheel perpendicularly to the axis of rotation, in order to measure the circumferential deformation, as shown in Figure 9.

Moreover, the experimental tests were performed by using SKF F 90 elastomeric joints, in order to reduce the noise interference up to 2-3μS.

In Figure 10, a comparison between experimental and numerical normal strains vs. normalized time at the base of tooth 25 of the pinion rotor is presented. The normalized time for the numerical analyses was modified in order to check the accuracy of the experimental measurements.

From Figure 10 it can be observed that the experimental tests give the same normal strain behaviour of the numerical FEM analyses: a peak of normal strain at the base of the contact tooth is found around the contact time (from 0.4 to 0.5), preceded and followed by a low constant value of normal strain. The normalized time is given along the x-axis (from 0.2 to 0.8) and the micro-strains με are given along the y-axis. It must be observed that the experimental maximum peak (+240με) is close to the corresponding numerical value (+220με).

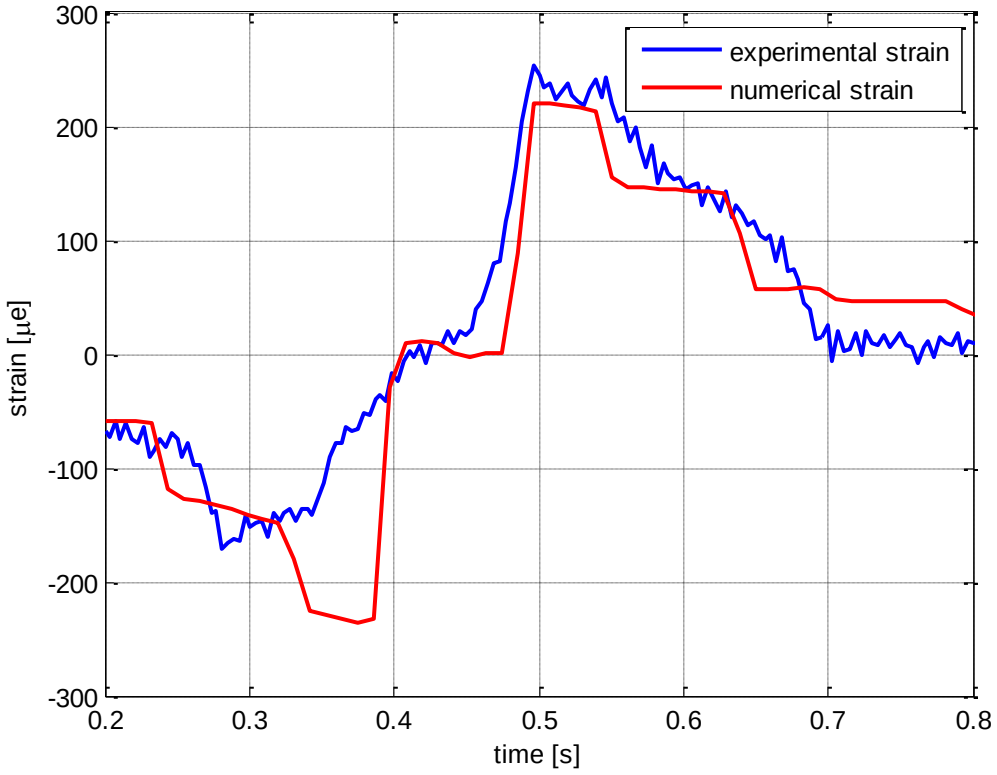

Figure 10: Comparison between experimental and numerical normal strains vs. normalized time at the base of tooth 25 of the pinion rotor.

4. Conclusions

In this paper, the normal strain distribution and pitting phenomenon on gear teeth are studied by means of numerical finite element analyses and experimental activities.

Experimental tests for the investigation of the pitting phenomenon in industrial gears are made at a specific nominal load (130Nm) and far from the resonance (840RPM). The experimental data are collected periodically from tri-axial accelerometers placed on the gear shafts. After a 4 hour test, a visible pitting phenomenon arises, with the presence of two big craters on the side of two adjacent teeth of the pinion, together with several smaller pits. The pitting phenomenon is given in four teeth (4,8,9,12), where for each pitted tooth the pitting sizes are 3.3%, 4.4%, 2%, 1.1%, respectively.

Numerical finite element studies on the normal strain distribution at the base of the gear teeth during the contact are performed. These studies are made at the same nominal load of the previous pitting analyses (130Nm) and at very low rotational speed (10RPM). A peak of normal strain at the base of the contact tooth is found around the contact time, preceded and followed by a low constant normal strain. The minimum peak is equal to -240με, the maximum peak is equal to +220με. The numerical results are validated by comparisons with experimental tests carried out considering the same operating conditions and placing strain gauges at the root fillet of six consecutive gear teeth; the strain gauges are mounted to measure the circumferential deformation at the tooth base; the acquisition data system is connected with the strain gauges on the two gears; elastomeric joints are used to reduce the noise interference. The experimental maximum peak of normal strain (+240με) is close to the corresponding numerical value.

REFERENCES

1 Fukumasu, N.K., Machado, G.A.A., Souza, R.M. and Machado, I.F., Stress Analysis to Improve Pitting Resistance in Gear Teeth, *Proceedings of the 3rd CIRP Conference on Surface Integrity*, Charlotte, NC, USA, 8-10 June, (2016).

2 Choy, F.K., Polyshchuk, V., Zakrajsek, J.J., Handschuh, R.F. and Townsend, D.P., Analysis of the effects of surface pitting and wear on the vibration of a gear transmission system, *Tribology International*, 29, 71-83, (1996). http://dx.doi.org/10.1016/0301-679X(95)00037-5

3 Faggioni, M., Samani, F., Bertacchi, G., Pellicano, F., Dynamic optimization of spur gears, *Mechanism and Machine Theory*, 46, 544-557, (2011). http://dx.doi.org/10.1016/j.mechmachtheory.2010.11.005

4 Del Rincon, F., Viadero, F., Iglesias, M., de-Juan, A., Garcia, P. and Sancibrian, R., Effect of cracks and pitting defects on gear meshing, *Proceedings of the IMechE Part C: Journal of Mechanical Engineering Science*, 226, 2805-2815, (2012).

5 Bonori, G., Barbieri, F., Pellicano, F., Optimum profile modifications of spur gears by means of genetic algorithms, *Journal of Sound and Vibration*, 313, (2008). http://dx.doi.org/10.1016/j.jsv.2007.12.013

6 Strozzi, M., Pellicano, F., Nonlinear vibrations of functionally graded cylindrical shells, *Thin-Walled Structures*, 67, 63-77, (2013). http://dx.doi.org/10.1016/j.tws.2013.01.009

7 Strozzi, M., Manevitch, L.I., Pellicano, F., Smirnov, V.V., Shepelev, D.S., Low-frequency linear vibrations of single-walled carbon nanotubes: Analytical and numerical models, *Journal of Sound and Vibration*, 333, 2936-2957, (2014). http://dx.doi.org/10.1016/j.jsv.2014.01.016

8 Smirnov, V.V., Manevitch, L.I., Strozzi, M., Pellicano, F., Nonlinear optical vibrations of single-walled carbon nanotubes. 1. Energy exchange and localization of low-frequency oscillations, *Physica D: Nonlinear Phenomena*, 325, 1-12, (2016). http://dx.doi.org/10.1016/j.physd.2016.03.015

9 Strozzi, M., Smirnov, V.V., Manevitch, L.I., Milani, M., Pellicano, F., Nonlinear vibrations and energy exchange of single-walled carbon nanotubes. Circumferential flexural modes, *Journal of Sound and Vibration*, 381, 156-178, (2016). http://dx.doi.org/10.1016/j.jsv.2016.06.013

10 Manevitch, L.I., Smirnov, V.V., Strozzi, M., Pellicano, F., Nonlinear optical vibrations of single-walled carbon nanotubes, *International Journal of Non-Linear Mechanics* (2016). Article in press. ISSN: 0020-7462. http://dx.doi.org/10.1016/j.ijnonlinmec.2016.10.010